Journal of Luminescence 168 (2015) 20–25

Contents lists available at ScienceDirect

Journal of Luminescence

journal homepage: www.elsevier.com/locate/jlumin

Nature of red luminescence in oxygen treated hydrothermally grown zinc oxide nanorods

Suranan Anantachaisilp [a,b], Siwaporn Meejoo Smith [b], Cuong Ton-That [a], Soraya Pornsuwan [b], Anthony R. Moon [a], Christian Nenstiel [c], Axel Hoffmann [c], Matthew R. Phillips [a,*]

[a] School of Mathematical and Physical Sciences, University of Technology Sydney, Broadway, NSW 2007, Australia
[b] Department of Chemistry, Faculty of Science, Mahidol University, Rajathevi, Bangkok 10400, Thailand
[c] Institut für Festkörperphysik, Technische Universität Berlin, Hardenbergstr. 36, 10623 Berlin, Germany

ARTICLE INFO

Article history:
Received 31 March 2015
Received in revised form
19 July 2015
Accepted 20 July 2015
Available online 29 July 2015

Keywords:
ZnO nanorods
Red luminescence emission
Hydrothermal growth

ABSTRACT

A strong broad red luminescence (RL) peak centered at 1.69 eV (FWHM=0.57 eV) at 15 K [1.78 eV (FWHM=0.69 eV) at 300 K] is formed in ZnO nanorods hydrothermally grown at low temperature following thermal annealing at 650 °C for 30 min in an O_2 gas environment. The optical properties of this peak were comprehensively studied using a range of characterization techniques, including photoluminescence and cathodoluminescence spectroscopy, X-ray absorption near edge spectroscopy and electron paramagnetic resonance spectroscopy. With decreasing temperature the RL peak position red shifted and its FWHM became narrower in accordance with the configuration coordinate model. Using these results, the RL has been assigned to highly lattice coupled V_{Zn}-related acceptor-like centers. No correlation was found between the observed red luminescence and nitrogen impurities.

1. Introduction

ZnO has attracted considerable attention in recent years as a promising material in a variety of technologically important optoelectronic devices and sensor applications [1–3]. Of particular importance is the luminescence of ZnO with optical emission that spans the ultra-violet, visible and near infrared spectral range. In the ultra-violet the emission is dominated by radiative near band edge (NBE) recombination mechanisms including, free and bound excitons as well as free-to-bound and donor-acceptor pair transitions involving shallow defects. While deep level defects produce broad emission peaks via a variety of recombination and internal mechanisms in the green (~2.5 eV and 2.3 eV) [4–7], yellow (~2.1 eV) [8–10], orange (~1.9 eV) [11] and red (1.7 eV) [8,12,13] at 300 K.

Despite considerable research effort unequivocal assignment of these luminescence peaks to specific dopants, impurities as well as defects and their complexes has not been realized up to now. Nevertheless there is general agreement that oxygen (V_O) and zinc (V_{Zn}) vacancies and interstitials (O_i and Zn_i) play a major role in these luminescence processes in undoped ZnO. To date most optical characterization studies have focused on the green luminescence and to a lesser extent the yellow and orange emission in ZnO. However, there is currently growing interest in the red luminescence (RL) for a number of reasons. First, it has been recently suggested that the RL could be a signature emission for N acceptors in ZnO [13] which is of importance to the development of stable p-type material. However, RL has also been attributed to zinc vacancies (V_{Zn}) [8,14], oxygen interstitials (O_i) [11,12], oxygen vacancies (V_O) [15] as well as the Zn_i–V_O complex or $V_{Zn}V_O$ divacancies [16]. Second, gas sensor studies have revealed a significant enhancement in the electrical sensitivity of the ZnO surface to specific target gases, such as NH_3, when RL dominates the luminescence spectrum [17]. Finally, the second-order correlation [$g^2(0)=0.1$] of photons in the red–orange spectral range confirming single photon emission in ZnO has been recently reported [18,19].

In this work the temperature and power density dependence of the RL in ZnO have been systematically investigated using cathodoluminescence spectroscopy. These data have been compared to ESR and photoluminescence NBE spectroscopy results as well as Electron Spin Resonance (ESR) and X-ray Absorption Near Edge Spectroscopy (XANES) data. Collectively these correlative studies

* Corresponding author.
E-mail addresses: siwaporn.smi@mahidol.ac.th (S.M. Smith), matthew.phillips@uts.edu.au (M.R. Phillips).

http://dx.doi.org/10.1016/j.jlumin.2015.07.025
0022-2313/

indicate that the RL is associated with highly lattice coupled V_{Zn}-related acceptor-like radiative recombination centers.

2. Samples and experiments

2.1. Fabrication and post growth processing of ZnO nanorods

Zinc acetate solution (5 mM in ethanol) was dropped on a silicon wafer to induce ZnO nucleation and then baked at 250 °C in air for 20 min. ZnO nanorods were grown using a hydrothermal treatment by placing the nucleated substrates in seed aqueous mixture containing 0.025 M zinc nitrate hexahydrate and 0.025 M hexamethylenetetramine at 90 °C for 3 h [20,21]. Analytical reagent grade zinc acetate dihydrate (> 98%, $(C_2H_3O_2)_2Zn \cdot 2H_2O$), zinc nitrate hexahydrate, (98%, $Zn(NO_3)_2 6H_2O$), and hexamethylenetetramine (HMT, ≥ 99.0%, $C_6H_{12}N_4$) from Aldrich were employed as received with no further purification. The as-grown nanorod samples were annealed at 650 °C for 30 min in O_2 gas environment. Hydrogen plasma treatment was conducted at a sample temperature of 100 °C using a mild 10 W hydrogen radio-frequency plasma for 20 min with 10 sccm H_2 flow rate.

2.2. Characterization of hydrothermally grown ZnO Nanorods

2.2.1. Cathodoluminescence

Cathodoluminescence (CL) spectra were collected using a FEI Quanta 200 scanning electron microscope equipped with the option of either an Ocean Optics QE6500 system or a Hamamatsu S7011-1007 CCD sensor. The Ocean Optics QE65000 system provides CL collection from 300 to 1000 nm with a spectral resolution of 0.9 nm. CL was collected by a diamond machined parabolic mirror positioned above the sample with an aperture to facilitate transmission of the electron beam. In temperature resolved experiments, the sample was placed on a liquid helium cold stage with the temperature varying from approximately 12 K to 300 K. In all CL experiments, the accelerating voltage of the electron beam was 5 kV which corresponds to a maximum photon generation depth of around 37 nm [22]. The electron beam current was varied from around 0.013 nA to 2.54 nA in power-density measurements. All CL spectra were corrected for the total response of the light collection system

2.2.2. Photoluminescence

High resolution PL was done utilizing the fourth harmonic generation (266 nm) of a Nd:YAG laser. A monochromator with a 1200 lines/mm grating (spectral resolution 0.2 meV) was used to disperse the emitted light. In temperature resolved experiments, the PL measurements were performed in a liquid helium bath cryostat allowing measurements from 7 K to 300 K. A HeCd Laser with the 325 nm emission line and an output power of 36 mW was used to excite the ZnO samples above the band gap. The emitted light was dispersed by a Spex-1404 double monochromator (spectral resolution 50 μeV) and detected by a bi-alkali photodetector.

2.2.3. X-Ray absorption near edge spectroscopy (XANES)

Total Fluorescence Yield (TFY) and Total Electron Yield (TEY) mode XANES analysis were performed around the N *K*-edge on the soft X-ray Spectroscopy beamline at the Australian Synchrotron. The incident X-ray beam was linearly polarized and perpendicular to the substrate surface. The photon energy scale was calibrated against the Au $4f_{7/2}$ peak at 84 eV from a clean gold film in electrical contact with samples.

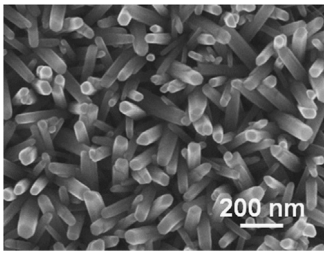

Fig. 1. SEM image of the as-grown < 0001 > ZnO nanorod ensemble, showing that the low temperature hydrothermal growth treatment produced a high density of uniform hexagonal < 0001 > nanorods approximately 55 nm in diameter orientated at different angles to the normal direction of the substrate.

2.2.4. Electron spin resonance

The ESR spectra were collected using a Bruker Elexys E500 cw X-band ESR spectrometer equipped with an Oxford ITC605 temperature controller. All presented ESR spectra were measured at 10 K using a power of 2.0 mW at a frequency of 9.4 GHz and modulation amplitude of 5.0 G.

3. Results and discussion

The low temperature 90 °C hydrothermal growth technique produced a continuous high density film of ZnO nanorods approximately 55 nm in diameter and 2000 nm in length (Fig. 1). XRD analysis (not shown) confirmed that the ZnO nanorods have a hexagonal wurtzite structure (P63mc) with lattice constants of $a = 0.3249$ nm and $c = 0.5207$ nm and that their longitudinal axis was normal to the c-plane. The < 0001 > ZnO nanorod ensemble are oriented at various angles to the normal direction of the substrate plane. No change in the crystal structure, morphology or orientation of the ZnO nanorods was observed after annealing at 650 °C in either O_2 or Ar.

Fig. 2(a) shows before and after annealing CL spectra at 300 K from the "as-grown" and O_2 heat treated nanorod films. The "as-grown" sample exhibits a ultra-violet peak centered at 3.17 eV arising from a number of highly overlapped thermally broadened LO-phonon replicas of the free exciton (FX) emission. A broad orange peak positioned at 1.99 eV is also observed in the as-grown nanorods. which has been previously attributed to Lithium acceptors [23] and O_i related centers [19]. After annealing in O_2 at 900 °C the NBE emission increases in intensity by a factor of 5 due to a thermally induced improvement in the quality of the ZnO nanorods following a reduction in the number of point and extended defects that provide non-radiative recombination pathways. Additionally and more significantly the O_2 heat treatment created a strong, highly symmetric red luminescence at 1.78 eV and FWHM of 0.69 eV. Fig. 2(b) shows that this emission was found to rapidly quench following exposure to a mild H_2 plasma strongly suggesting that the chemical origin of the RL is related to acceptor-like centers as hydrogen is a well-known donor in ZnO. The accompanying large increase in the NBE could indicate that the RL center acts as an efficient competitive recombination channel to the NBE, however, further H passivation of non-radiative pathways cannot be ruled out. At 15 K the RL peak position, see Fig. 2(c), slightly red shifts to 1.69 eV and the FWHM narrows to 0.57 eV, which can be interpreted by a configurational coordinate (CC) model [24]. Furthermore the absence of any fine structure in the peak at 15 K eliminates the assignment of the observed RL to transition metal impurities, such as Fe, Co and Ni, which exhibit characteristic sharp features due to internal 3d transitions [25,26]. The presence of a broad emission at 2.5 eV has been attributed to surface and bulk V_O centers at 5 K [19,27]. In addition at 15 K the NBE blue